

NANOSTRUCTURES

PACS numbers: 61.46.–w; 42.65.Dr; 42.62.Fi; 79.20.Eb
DOI: 10.1070/QE2012v042n03ABEH014761

Au-coated ZnO nanostructures for surface enhanced Raman spectroscopy applications *

A.Og. Dikovska, N.N. Nedyalkov, S.E. Imamova, G.B. Atanasova, P.A. Atanasov

Abstract. **Thin ZnO nanostructured films were produced by pulsed laser deposition (PLD) for surface enhanced Raman spectroscopy (SERS) studies. The experimental conditions used for preparation of the samples were chosen to obtain different types of ZnO nanostructures. The Raman spectra of rhodamine 6G (R6G) were measured at an excitation wavelength of 785 nm after coating the ZnO nanostructures with a thin Au layer. The influence of the surface morphology on the Raman signal obtained from the samples was investigated. High SERS signal enhancement was observed from all Au-coated ZnO nanostructures.**

Keywords: *ZnO nanostructured films, surface enhanced Raman spectroscopy, pulsed laser deposition.*

1. Introduction

Surface enhanced Raman spectroscopy (SERS) can ensure a breakthrough in the sensitivity of chemical, biological and environmental sensing devices due to a considerable increase in Raman signals although the Raman cross section is inherently very small. The advantages offered by nanotechnologies have additionally attracted the attention of the scientific researchers to SERS effects in various nanostructures, such as Au nanoparticles [1, 2], Au nanoporous structures [3], flower-like Au nanostructures [4], etc. In addition, different oxide nanostructures covered by Au or Ag have also been investigated as suitable substrates for SERS analyses. For example, Sakano et al. [5] observed a high SERS enhancement factor from Au-coated ZnO nanorods.

ZnO nanostructures have attracted enormous interest due to their potential application in nanoscale electronics and photonics [6–8]. Among the various synthesis methods, pulsed laser deposition (PLD) has been proven to be a simple and effective catalyst-free method for preparation of nanoscale materials [9–12]. Several studies have been reported dealing with ZnO nanostructures grown by PLD and exploring a wide range of such experimental parameters as choice of substrate, substrate temperature, background oxygen pressure, etc. [10, 12, 13]. The use of a buffer ZnO layer as a possible way of supplying growth nuclei for the subsequent growth of ZnO nanostructures has also attracted current interest [10, 14]. It was demonstrated in [10, 14] that, once a buffer layer is introduced, the subsequent ZnO nanostructures growth can exhibit different morphologies. Our previous investigations also showed that the use of a buffer layer creates a new possibility to form a variety of morphologies and nanostructures [15].

In the present paper we report a study on nanostructured ZnO film fabrication by PLD and the measurements of the SERS characteristics of these samples after Au-coating. Rodamine-6G (R6G) was used as a SERS active molecule pumped at 785 nm. The influence of the surface morphology on the Raman response of the samples at a fixed R6G concentration was investigated.

2. Experimental

Thin ZnO films were prepared on an amorphous SiO_2 substrate by PLD. The third harmonic of a 355-nm Nd:YAG laser with a FWHM pulse duration of 18 ns and a repetition rate of 10 Hz was used for ablation of a ZnO ceramic target. The target-to-substrate distance was fixed at 40 mm in a standard on-axis configuration. All the experiments were performed in oxygen atmosphere. The substrate temperature was kept at 300 °C during deposition.

The nanostructured films were fabricated via a two step process. As a first step, a thin ZnO film was prepared at a high oxygen pressure in order to form growth nuclei. Oxygen pressures of 20, 50, and 100 Pa were used for preparation of three different types of nuclei. The laser fluence was kept constant at 2 J cm^{-2}. The second step consisted in the deposition of a ZnO film on the created nuclei. At this stage, the oxygen pressure was decreased to 5 Pa and kept constant to the end of the experiment. During the second step, laser fluence was 3.5 J cm^{-2}.

A smooth ZnO film was also prepared as a reference for SERS analysis. The smooth ZnO surface with a root-mean-square (RMS) value of a few nanometers was deposited at an oxygen pressure of 5 Pa as described elsewhere [16].

The surface morphology of the ZnO nanostructured sample was analysed using a JEOL JSM-5510 scanning electron microscope (SEM). Atomic force microscopy (AFM) measurements (Agilent 5500) were also performed in order to characterise the grain size of the samples [17]. The deposited samples were coated with a thin Au layer produced by cathode sputtering in order to prepare the samples for SERS analysis. The SERS spectra of the Au-coated ZnO nanostructures

* Reported at the XIX International Conference on Advanced Laser Technologies (ALT'11), Bulgaria, Golden Sands, September 2011.

A.Og. Dikovska, N.N. Nedyalkov, S.E. Imamova, P.A. Atanasov Institute of Electronics, Bulgarian Academy of Sciences, 72 Tsarigradsko Chaussee, Sofia 1784, Bulgaria; e-mail: dikovska@ie.bas.bg;
G.B. Atanasova Institute of General and Inorganic Chemistry, Bulgarian Academy of Sciences, 'Acad. G. Bonchev str.', bld. 11, 1113 Sofia, Bulgaria

Received 27 October 2011; revision received 16 December 2011
Kvantovaya Elektronika **42** (3) 258–261 (2012)
Submitted in English

were investigated using a DeltaNu Raman spectrometer with an attached microscope (NuScope). The 60-mW Raman apparatus operating at an excitation wavelength of 785 nm had a laser spot with diameter of 100 μm.

For the R6G measurements, 12 mg of rhodamin-6G was dissolved in 300 mL of ethanol in a plastic bottle in order to obtain a concentration of 10^{-6} M. The total number of R6G molecules in one drop (20 μL) placed on the Au-coated nanostructures was approximately $\sim 1 \times 10^{13}$. The molecules were distributed on an area of 1 cm^2. Each spot with an area of 1 μm^2 contained about $\sim 1 \times 10^5$ R6G molecules.

3. Results and discussion

The surface morphology is a very important parameter affecting the formation of nanostructures. The rough crystal surface plays the role of nuclei for nanostructured film growth [18]. Therefore, our first step during the nanostructure preparation was formation of a thin ZnO layer with a clearly pronounced rough surface. As is well known, the films prepared at a higher oxygen pressure exhibit a rough surface with a high peak-to-valley ratio [16]. Thus, layers with thickness lower than 50 nm were deposited at three different oxygen pressures in order to create different types of growth nuclei. In the second step, ZnO was deposited on the created nuclei. The ZnO growth follows the nuclei during PLD and then a nanostructured film is formed.

The AFM images of the deposited ZnO nanostructures are presented in Fig. 1. The surface morphology of the sample presented in Fig. 1a contains grains (the mean grain size in the range 60–110 nm) with clearly pronounced spherical morphology. The grains are packed closely and well-distributed on the substrate with RMS surface roughness of about 10 nm. The scale bar in the AFM image (Fig. 1a) indicates a high peak-to-valley ratio. This value is higher compared with the value obtained for the film deposited when the oxygen pressure of 20 Pa was kept constant during the entire deposition process [16]. It is worth pointing out that the ZnO buffer layer deposited at 20-Pa oxygen pressure has the crystal structure reported in our previous investigations [16]. The growth of the ZnO nanostructure follows the crystal nuclei. The surface morphology of the sample prepared by a ZnO buffer layer deposited at 50 Pa is presented in Fig. 1b. The increase in the oxygen pressure applied during the buffer layer deposition leads to a change in the surface morphology. It consists of a nonuniform structure with a larger grain size (100–200 nm), in contrast with the sample shown in Fig. 1a. Additionally, the increase in the oxygen pressure worsens the crystal structure of the buffer layer. The further increase in the oxygen pressure applied during the buffer layer deposition (100 Pa) preserves the nonuniform structure of the surface morphology (Fig. 1c). In this case, the sample grain size ranges from 100 to 200 nm. Furthermore, the prepared buffer layer is almost amorphous at this high oxygen pressure.

The SEM images of the Au-coated ZnO nanostrucures are presented in Fig. 2. The sample presented in Fig. 2a shows a uniform densely packed structure with small grains, which confirms the results obtained by AFM imaging. Moreover, no significant difference is observed in the surface morphology of the samples prepared at higher oxygen pressures (50 and 100 Pa) after Au-coating (Figs 2b and c).

High SERS enhancement factor practically means spatial inhomogeneity. The enormous SERS effects usually occur in the so-called 'hot sites', i.e., very small volumes in the cavities

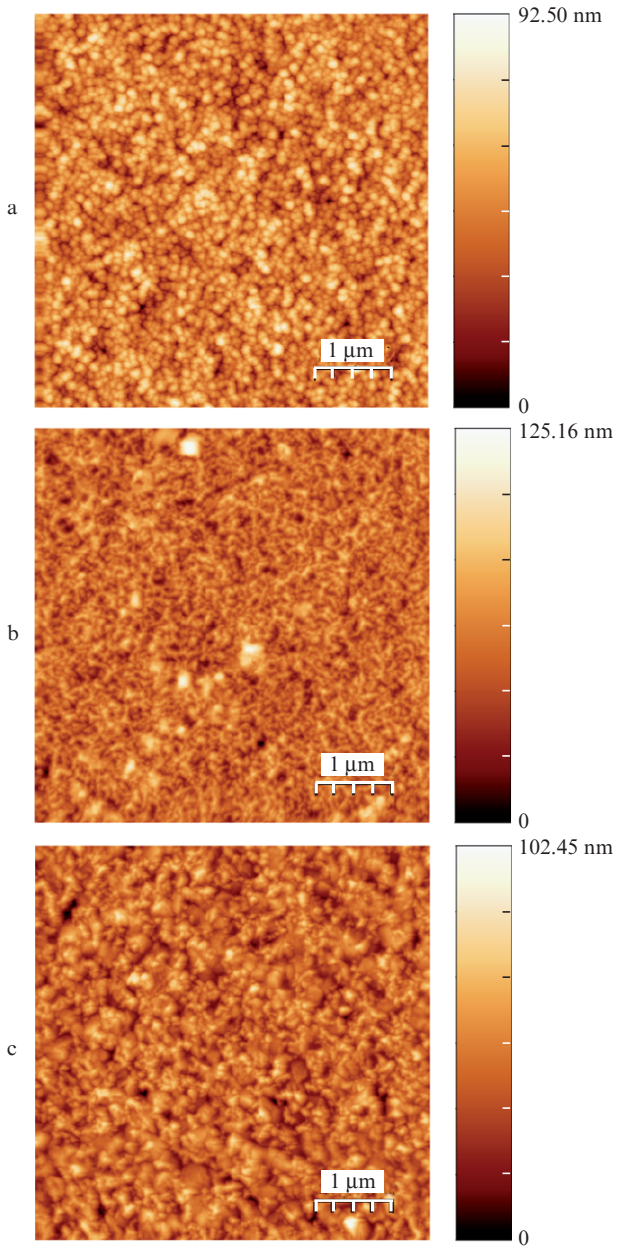

Figure 1. AFM images of ZnO nanostructured films prepared on the basis of different nuclei at oxygen pressures of (a) 20 Pa, (b) 50 Pa, and (c) 100 Pa during deposition.

between metal nanoparticles [19–21]. Theoretical studies show that the local electromagnetic field near metal nanoparticles is strongly confined to the 'hot sites' by the surface plasmon resonance resulting in an inhomogeneous electromagnetic energy distribution [22]. Since metallic nanoparticle arrays supply a high density of nanocavities between particles, i.e., SERS 'hot sites', they seem to be the perfect substrates for SERS. To this end, the ZnO nanostructures after Au-coating were additionally tested to study their suitability as substrates for SERS measurements taking into account their morphology shown in Fig. 2.

The SERS spectra of Au-coated ZnO samples are presented in Fig. 3. Strong peaks at 610, 772, 1182, 1303, 1360, and 1505 cm^{-1} were attributed to the Raman spectrum of the R6G molecules. The intensity of the Raman signals was compared with the reference signal obtained from Au-coated

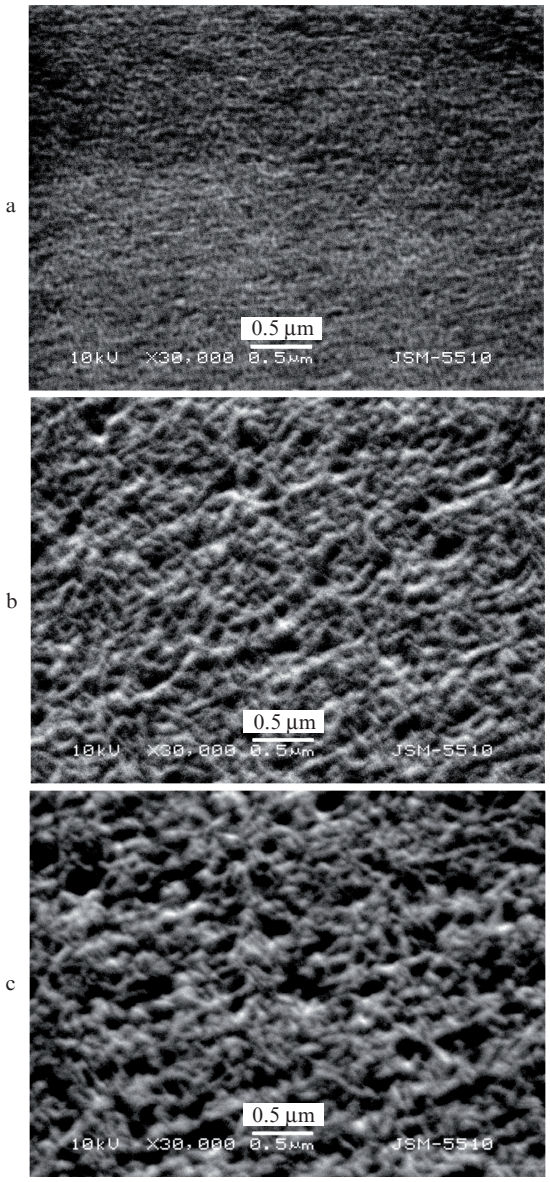

Figure 2. SEM images of the Au-coated ZnO nanostructured films prepared on the basis of different nuclei at oxygen pressures of (a) 20 Pa, (b) 50 Pa, and (c) 100 Pa during deposition.

smooth ZnO film with R6G. As expected, no signal was registered from the Au-coated smooth surface (see Fig. 3), which proves that Au-coated nanostructures are suitable for SERS applications. The highest signal intensity was obtained from the sample prepared with a buffer layer deposited at 20-Pa oxygen pressure [Fig. 3, curve (*1*)]. This result is the consequence of the small grain-size structure of the sample (see Fig. 1a). The use of Au-coated ZnO nanostructures with larger grains, such as the samples shown in Figs 1b and c, led to registration of Raman peaks with lower intensity. It is worth noting that the tendency of decreasing the intensity of the Raman peaks is preserved as the grain size is increased. This result is in good agreement with previous reports [23]. The dependence observed is related to the higher density of the spatial inhomogeneities realised in the film with the smallest grain size. In addition, the evanescent nature of the near field ensures strong intensity enhancement in gaps with sizes

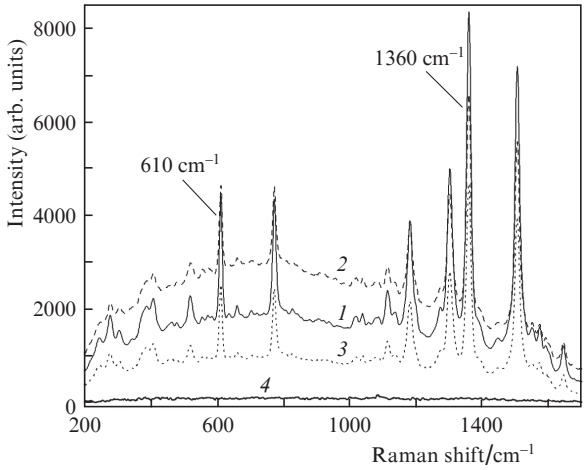

Figure 3. SERS spectra of Au-coated ZnO nanostructured samples prepared at oxygen pressures of (*1*) 20 Pa, (*2*) 50 Pa, and (*3*) 100 Pa used for formation of the growth nucei. The reference signal (*4*) was obtained from Au-coated smooth ZnO film.

of only few nanometres. The intensity drops rapidly with increasing gap distance.

The Raman spectra of the Au-coated ZnO nanostructures with R6G were compared with the bulk R6G Raman spectrum in order to estimate the enhancement factor (EF). The normal Raman signal of R6G molecules is presented in Fig. 4. Only the peaks at 610 and 1360 cm^{-1} were attributed to the R6G molecules. All other peaks in the figure belong to ethanol. Therefore, the weak peaks only observed at 610 and 1360 cm^{-1} in the normal Raman spectrum allowed the evaluation of the EF. For EF evaluation the following equation was used:

$$\mathrm{EF} = \frac{I_{\mathrm{sers}} N_{\mathrm{bulk}}}{I_{\mathrm{bulk}} N_{\mathrm{sers}}}. \qquad (1)$$

where I_{sers} and I_{bulk} are the peak intensities of the SERS and bulk spectra; N_{sers} and N_{bulk} are the number of molecules used in N_{sers} and bulk measurements, respectively. The value of N_{sers} was calculated to be approximately 7×10^8 for laser spot

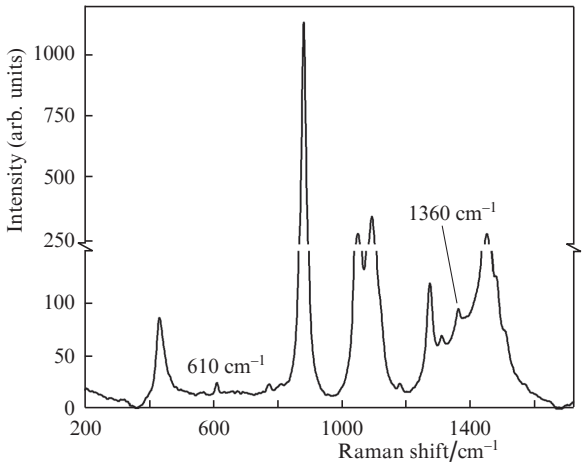

Figure 4. Normal Raman spectra of rodamin-6G molecules, dissolved in ethanol, excited at 785 nm.

of diameter 100 μm and $N_{bulk} \sim 8 \times 10^{12}$. The ratio N_{bulk}/N_{sers} was equal to $\sim 1 \times 10^4$. The intensities I_{sers} and I_{bulk} normalised to the incident laser photon flux were determined using the Raman spectra presented in Figs 3 and 4. The ratio between the maximum and the minimum for the highest peaks changed by a factor of 3 to 5 in the SERS spectra, as is shown in Fig. 3, while for the normal Raman spectrum this ratio was about one. Finally, the EF calculated using Eqn (1) for the Au-coated ZnO nanostructures was approximately $10^6 - 10^7$, i.e., the SERS sensitivity of the gold nanostructured films is quite high. However, it should be noted that in our experiment the Raman scattering by R6G molecules is nonresonant. The resonant Raman scattering which is at 530 nm for R6G molecules may increase the EF by more than 1000 times.

4. Conclusions

Nanostructured ZnO films were prepared for SERS application. The Raman spectra of rhodamine 6G were measured at an excitation wavelength of 785 nm after coating the ZnO nanostructures with a thin Au layer. The highest Raman intensity obtained from the sample prepared with a buffer layer deposited at a 20-Pa oxygen pressure resulted from the small grain-size structure obtained. The SERS spectra were compared with the Raman spectra of an Au-coated smooth ZnO film, as well as with the normal Raman spectra of R6G molecules. An enhancement factor of approximately $10^6 - 10^7$ was evaluated for all Au-coated ZnO nanostructures with R6G.

Acknowledgements. This work was supported in part by the Bulgarian Ministry of Education and Science (Contract No. DO 02-293/08). The authors would like to thank M. Stankova from Universitat Rovira i Virgili, Spain, for the AFM measurements.

References

1. Félidj N., Aubard J., Lévi G., Krenn J.R., Hohenau A., Schider G., Leitner A., Aussenegg F.R. *Appl. Phys. Lett*., **82**, 3095 (2003).
2. Duan G., Cai W., Luo Y., Li Y., Lei Y. *Appl. Phys. Lett*., **89**, 181918 (2006).
3. Qian L.H., Yan X.Q., Fujita T., Inoue A., Chen M.W. *Appl. Phys. Lett*., **90**, 153120 (2007).
4. Duan G., Cai W., Luo Y., Li Z., Li Y. *Appl. Phys. Lett*., **89**, 211905 (2006).
5. Sakano T., Tanaka Y., Nishimura R., Nedyalkov N.N., Atanasov P.A., Saiki T., Obara M. *J. Phys. D: Appl. Phys*., **41**, 235304 (2008).
6. Huang M.H., Wu Y., Feick H., Tran N., Weber E., Yang P. *Adv. Mater*., **13**, 113 (2001).
7. Lui Z.W., Ong C.K., Yu T., Shen Z.X. *Appl. Phys. Lett*., **88**, 053110 (2006).
8. Park S.-H., Kim S.-H., Han S.-W. *Nanotechnol*., **18**, 055608 (2007).
9. Nishimura R., Sakano T., Okato T., Saiki T., Obara M. *Jpn. J. Appl. Phys*., **47**, 4799 (2008).
10. Sun Y., Fuge G.M., Ashfold M.N.R. *Superlattice Microst*., **39**, 33 (2006).
11. Hartanto A.B., Ning X., Nakata Y., Okada T. *Appl. Phys. A*, **78**, 299 (2004).
12. Sun Y., Doherty R.P., Warren J., Ashfold M.N.R. *Chem. Phys. Lett*., **447**, 257 (2007).
13. Okada T., Agung B.H., Nakata Y. *Appl. Phys. A*, **79**, 1417 (2004).
14. Conley J.F., Stecker L., Ono Y. *Nanotechnol*., **16**, 292 (2005).
15. Dikovska A.Og., Atanasova G.B., Nedyalkov N.N., Stefanov P.K., Atanasov P.A., Karakoleva E.I., Andreev A.Ts. *Sens&Act. B*, **146**, 331 (2010).
16. Dikovska A.Og., Atanasov P.A., Vasilev C., Dimitrov I.G., Stoyanchov T.R. *J. Optoelectron.&Adv. Mater*., **7**, 1329 (2005).
17. Horcas I., Fernández R., Gómez-Rodríguez J.M., Colchero J., Gómez-Herrero J., Baro A.M. *Rev. Sci. Instr*., **78**, 013705 (2007).
18. Xia Y., Yang P., Sun Y., Wu Y., Mayers B., Gates B., Yin Y., Kim F., Yan H. *Adv. Mater*., **15**, 353 (2003).
19. Xu H.X., Bjerneld E.J., Käll M., Börjesson L. *Phys. Rev. Lett*., **83**, 4357 (1999).
20. Xu H.X., Aizpurua J., Käll M., Apell P. *Phys. Rev. E*, **62**, 4318 (2000).
21. Michaels A.M., Jiang J., Brus E. *J. Phys. Chem. B*, **104**, 11965 (2000).
22. Imamova S., Dikovska A., Nedyalkov N., Atanasov P., Sawczak M., Jenrizejewski R., Sliwinski G., Obara M. *J. Optoelectron.&Adv. Mat*., **12**, 500 (2010).
23. Hossain M.K., Shibamoto K., Ishioka K., Kitajima M., Mitani T., Nakashima S. *J. Lumin*., **122-123**, 792 (2007).